ISSN 2176-5480

22nd International Congress of Mechanical Engineering (COBEM 2013)
November 3-7, 2013, Ribeirão Preto, SP, Brazil

ON THE USE OF RESONANCE TO DISCARD SATELLITES OF GNSS

Diogo Merguizo Sanchez
National Institute for Space Research, INPE, São José dos Campos, SP, Brazil
sanchezfisica@gmail.com

Tadashi Yokoyama
State University of São Paulo, UNESP, Rio Claro, SP, Brazil
tadashi@rc.unesp.br

Antonio Fernando Bertachini de Almeida Prado
National Institute For Space Research, INPE, São José dos Campos, SP, Brazil
prado@dem.inpe.br

Abstract. *The current strategy for the discard of satellites of the Global Navigation Satellite Systems (GNSS) is to place these satellites in disposal orbits 500 km above and below of the nominal orbit. However, in doing that, due to the fast increasing of the population in this region, a potential problem appears due to the real possibility of collisions among these disposal satellites, which will generate significant and unwanted debris. Several studies have been made to develop alternative strategies to mitigate this problem. In this work, we propose simple, but efficient techniques exploiting Hohmann type maneuvers combined with the use of the 2:1 resonance between the argument of perigee and the longitude of the ascending node, to increase the orbital eccentricity of the satellite, promoting atmospheric reentrance. The results are showed in terms of the increment of velocity necessary to transfer the satellites to new orbits. Some comparisons with direct discarding maneuvers (Hohmann type) are also presented. We use the exact equations of motion, considering the perturbations of the Sun, the Moon, and the solar radiation pressure. The geopotential model was considered up to order and degree four.*

Keywords: *GNSS, disposal orbits, inclination resonance, luni-solar perturbation.*

1. INTRODUCTION

Global Navigation Satellite Systems is a general denomination for constellations of navigation satellites, such as GPS (USA), Glonass (Russian), Galileo (European), and Beidou (Chinese). The GPS has 31 active satellites in orbits with altitude near 20,000 km and 56 degrees of inclination. This value of the inclination is the same one used for the Galileo system (four active satellites, with approximately 23,000 km of altitude). The Beidou system has 15 satellites, but only one in MEO (Medium Earth Orbit) with inclination about 56°. The remaining satellites are in GEO (Geosynchronous Earth Orbit), with inclinations about one degree (9 satellites) and 55° (5 satellites). The Glonass system has 31 active satellites with inclinations ranging between 63° and 65°, and 19,129 km of altitude. We will not consider the Glonass system in this work, as well the Beidou satellites with inclination of one degree, because our technique is mainly devoted for satellites with inclinations around 56°, region where the 2:1 resonance is very efficient.

An important characteristic of the GNSS satellites that are in MEO is the effect of the J_{22} and the J_{32} harmonics of the geopotential, which cause short periodic variations in the semi-major axis (Vilhena de Moraes *et al*., 1995; Ferreira and Vilhena de Moraes, 2009). This fact occurs because these satellites are in the vicinity of the 2:1 resonance between the orbital period of the satellite and the spin of the Earth. In general, the tesseral harmonics induce perturbations with short period and low amplitude in the orbital motion of the satellites. However, in the presence of this specific 2:1 resonance, these terms may produce effects of high amplitude and long period (Allan, 1967; Rossi, 2008).

In this scenario, the current way to discard the satellites of the GNSS is to transfer the satellites to orbits that are 500 km above or below the nominal orbit (NASA, 1995). With the increase of the debris around the Earth and the discovery that these disposal orbits are potentially unstable (Chao, 2000; Gick and Chao, 2001), many efforts have been made to create new strategies and techniques to discard these satellites (Chao and Gick, 2004; Jenkin and Gick; 2005, Jenkin and Gick, 2006; Sanchez *et al*., 2009; Pardini and Anselmo, 2012). From the analysis of the initial conditions which lead to the previously mentioned instability (a significant growth of eccentricity), caused by the 2:1 resonance between the argument of perigee (ω) and the longitude of the ascending node (Ω), some works suggest to move the disposed satellites to regions such that the growth of the eccentricity does not allow the disposed satellites to invade the region of the operational satellites, at least for some acceptable time. This strategy may present certain inconveniences, such as an accumulation of objects in the disposal region, increasing the risk of collisions between disposed objects, generating a new source of hazardous debris.

On the other way, there are some works that suggest transferring the disposed satellites to appropriate orbits such that the new initial conditions lead to an increase of eccentricity. The main goal is to lower continuously the periapsis radius of the disposed satellites, provoking their entrance in the atmosphere of the Earth. A positive characteristic of this

ISSN 2176-5480

approach is the decrease in the number of space debris, so reducing the collisional risk between inactive objects. Although the increase of the eccentricity may lead to a possible increase in the collisional risk between disposed and active objects, this risk can be minimized with a proper choice of initial conditions, which can accelerate the decay of these satellites. Therefore, the time that the satellite takes to reentry in the atmosphere is an important question related to the cost and success of this strategy.

Our study evaluates the use of the strategy of eccentricity growth under the effect of the 2:1 resonance between perigee and ascending node in comparison with the direct discard using a Hohmann type transfer. This comparison is shown in terms of the velocity increment necessary to perform the atmospheric reentry. For the strategy that uses the resonance, grids of initial conditions were generated to evaluate the maximum eccentricity reached by the satellites after 250 years considering their nominal altitudes and also considering an apoapsis radius 10,000 km above and below their nominal apoapsis radius. Testing different initial altitudes makes sense, since our purpose is to lower the periapsis of the orbit to drive the satellites to enter in the atmosphere within some pre-fixed time interval. We will see that these tests also show the "strength" of the resonance for different values of the semi-major axis of the orbit of the satellite, since, from the mathematical point of view, the 2:1 resonance between perigee and ascending node always exists, no matter what is the altitude of the satellite.

2. THE RESONANCE $2\dot{\omega} + \dot{\Omega} \approx 0$ AND ITS EFFECTS

For the GNSS satellites, usually the oblateness is the dominant part and the single averaged form (Sanchez *et al*., 2009) it is given by:

$$R_{J_2} = \frac{1}{4} n^2 J_2 R_P^2 (3cos^2(I) - 1)(1 - e^2)^{-3/2}, \quad (1)$$

where n is the mean motion of the satellite and R_P is the mean equatorial radius of the Earth.

In this case, the main frequencies of the system are given by:

$$\dot{\omega} \approx \frac{3nJ_2R_P^2}{4a^2(1-e^2)^2}(5cos^2(I) - 1), \quad (2)$$

$$\dot{\Omega} \approx -\frac{3nJ_2R_P^2}{2a^2(1-e^2)^2}cos(I). \quad (3)$$

The ratio between $\dot{\Omega}$ and $\dot{\omega}$ is:

$$\frac{\dot{\Omega}}{\dot{\omega}} \approx \frac{2cos(I)}{1-5cos^2(I)} = k. \quad (4)$$

For k = integer we have the special resonances which do not depend on the semi-major axis, as we said before. These resonances usually affect the eccentricity (Yokoyama, 1999). For $k = -2$ we have $2\dot{\omega} + \dot{\Omega} \approx 0$ for $I = 56.06°$ or $I = 110.99°$. Another classical resonance occurs when $I = 63.4°$, so that $\dot{\omega} \approx 0$.

The closer the inclination of the GNSS satellite is to 56.06°, the stronger will be the effect of the resonance on the eccentricity (Sanchez *et al*., 2009). In order to see the effects of this resonance, the osculating equations of motion of a satellite will be integrated. For the moment, as disturbers, we consider only the Sun and the oblateness of the Earth (the complete Cartesian equations involving the remaining disturbers will be given in the next section). Figure 1 shows the effects of the resonance on the eccentricity and on the resonant angle. Note that an initial small eccentricity reaches a significant increase.

ISSN 2176-5480

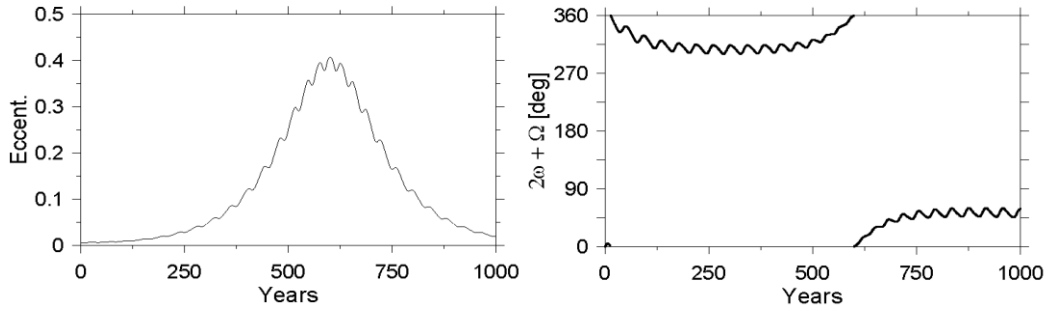

Figure 1. Time evolution of the eccentricity (left) and the critical angle (right). Initial conditions: a = 30,647 km, e = 0.005, I = 56.06° and other elements equal to zero. In the simulations we consider only the Sun and the oblateness of the Earth as disturbers.

For the inclination I = 56.06°, the dominant resonant term in the double averaged solar disturbing function ($\hat{R}_\odot$) is $cos(2\omega + \Omega - \Omega_\odot)$. Neglecting the remaining terms of $\hat{R}_\odot$ (a full development of the single and double averaged disturbing function of the Sun is found in Sanchez *et al.* (2009)), the Hamiltonian of the problem is:

$$F = R_{J_2} + \frac{k^2 M_\odot a^2}{2r_\odot^3}\left[\frac{P}{8}\left(1 - 3cos^2(I) - 3cos^2(I_\odot) + 9cos^2(I)cos^2(I_\odot)\right)\right.$$
$$\left. -\frac{3}{4}Zsin(I)sin(I_\odot)\big(1 + cos(I)\big)cos(I_\odot)cos(2\omega + \Omega - \Omega_\odot)\right], \quad (5)$$

where k is the gravitational constant, $M_\odot$ is the mass of the Sun and $r_\odot$, $I_\odot$, $\Omega_\odot$, are, respectively, the modulus of the position vector, the inclination and the ascending node of the Sun. $P = 1 + \frac{3}{2}e^2$ and $Z = \frac{5}{2}e^2$.

Taking $L = \sqrt{k^2(M_T + m)a}$, $G = L\sqrt{1 - e^2}$, $H = Gcos(I)$, l = mean anomaly, $\omega = g$, $\Omega = h$, the set of the Delaunay variables, and performing a Mathieu canonical transformation (Lanczos, 1970), we have:

$$\tilde{R}_\odot = \frac{k^2 M_\odot a^2}{2r_\odot^3}\left[\frac{P}{8}\left(1 - 3\frac{(P_1+P_2)^2}{4P_1^2} - 3cos^2(I_\odot) + 9\frac{(P_1+P_2)^2}{4P_1^2}cos^2(I_\odot)\right)\right.$$
$$\left. -\frac{3}{4}Z\left(1 - \frac{(P_1+P_2)^2}{4P_1^2}\right)^{\frac{1}{2}}sin(I_\odot)\left(1 + \frac{P_1+P_2}{2P_1}\right)cos(I_\odot)cos(\theta_1)\right], \quad (6)$$

$$\tilde{R}_{J_2} = \frac{1}{4}n^2 J_2 R_P^2\left(3\frac{(P_1+P_2)^2}{4P_1^2} - 1\right)\left(1 - \frac{L^2 - 4P_1^2}{L^2}\right)^{-\frac{3}{2}}. \quad (7)$$

where $\theta_1 = 2\omega + \Omega$, $P_1 = \frac{G}{2}$, $\theta_2 = \Omega$, $P_2 = H - \frac{G}{2}$.

The orbit of the Sun is assumed to be Keplerian and we also considered $\omega_\odot = 0$, $\Omega_\odot = 0$. In (P_i, θ_i) variables, our Hamiltonian is a one degree of freedom problem, whose dynamics is very similar to the Lidov-Kozai resonance. In Fig. 2 we consider an initial eccentricity e_0 = 0.005 and semi-major axis a = 30,647 km. This figure is very instructive: note that in the bottom part there is a large region where the satellite remains some finite time with very small eccentricity. It corresponds to the region where $2\omega +$ ≈ 0, which is the region of interest for the minimum eccentricity strategy study shown in Sanchez *et al.* (2009). On the other hand, we have the counterpart of this situation at the top of the figure: very high eccentricity, which occurs again for $2\omega +$ ≈ 0. This is our region of interest, because we intent to use this increase of eccentricity to discard the satellites. It is worth noting that, if the semi-major axis is high, the effect of the Moon cannot be neglected, so that the problem is no more a one degree of freedom problem. In this case the search of the (ω, Ω) pair such that the eccentricity increases must be done by integrating the complete equations of motion. A full characterization of this resonance is found in Sanchez *et al.* (2009).

The time that the eccentricity demands to reach high values is determinant to the utility of this resonance in the discard of the satellites. In the next section we will take into account this criterion in the search of initial conditions that causes an increase in the eccentricity.

ISSN 2176-5480

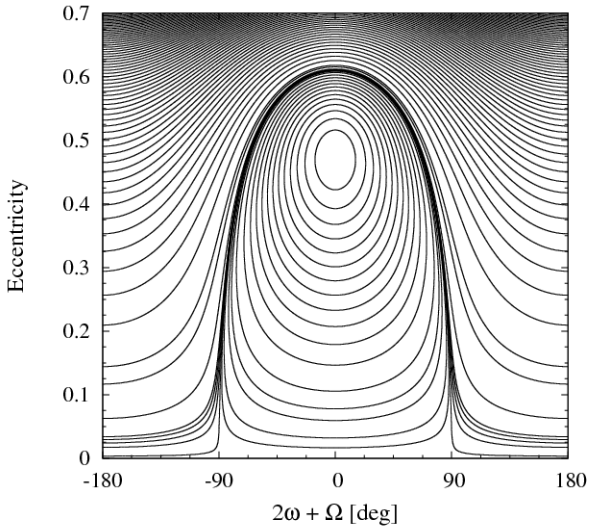

Figure 2. Level curves of the Hamiltonian ($\tilde{R}_{\odot} + \tilde{R}_{J_2}$), showing the eccentricity variation versus resonant angle.

3. INITIAL CONDITIONS FOR THE STRATEGY OF INCREASING THE ECCENTRICITY

In the previous section, we considered only the effects of the Sun and the oblateness of the Earth. Moreover, in the presence of the resonance, the main effects are now governed by the long term variations, since we considered the averaged problem. From a theoretical point of view, this averaged system is quite efficient to highlight the basic dynamics that affects the eccentricity of the GNSS satellites. However, for a more complete and realistic study we need to include more disturbers.

In this section we want to find some special initial conditions such that the eccentricity of the satellites reaches high values within an interval of 250 years. The strategy to search for these particular initial conditions is guided from the theoretical approach described in the previous section.

We integrate the exact equations of motion of a satellite to be disposed of the GNSS (which have inclination around 56°) under the effects of the Sun, the Moon, the oblateness of the Earth, and the radiation pressure coming from the Sun. We use the RADAU (Everhart, 1985) integrator written in FORTRAN language and compiled using a Linux system.

The acceleration of the satellite using the exact system is:

$$\ddot{\boldsymbol{r}} = -\frac{GM_T}{r^3}\boldsymbol{r} - GM_{\odot}\left(\frac{\boldsymbol{r}-\boldsymbol{r}_{\odot}}{|\boldsymbol{r}-\boldsymbol{r}_{\odot}|^3} - \frac{\boldsymbol{r}_{\odot}}{|\boldsymbol{r}_{\odot}|^3}\right) - GM_L\left(\frac{\boldsymbol{r}-\boldsymbol{r}_L}{|\boldsymbol{r}-\boldsymbol{r}_L|^3} - \frac{\boldsymbol{r}_L}{|\boldsymbol{r}_L|^3}\right) + \boldsymbol{P}_G + \boldsymbol{P}_{RP}, \tag{8}$$

where G is the gravitational constant, M_T, $M_{\odot}$, M_L are the masses of the Earth, the Sun and the Moon, respectively. $\boldsymbol{r}$, $\boldsymbol{r}_{\odot}$, $\boldsymbol{r}_L$ are, in order, the position vector of the satellite, the Sun and the Moon. $\boldsymbol{P}_G$ is the acceleration due to the disturbing geopotential up to order and degree 4x3, given by the GEM10 model (Kuga et al., 1983). $\boldsymbol{P}_{RP}$ is the acceleration due to the radiation pressure of the Sun, given by Mignard (1991), and Beugé and Ferraz-Mello (1994):

$$\boldsymbol{P}_{RP} = -K^* \frac{\boldsymbol{r}_{\odot}}{|\boldsymbol{r}_{\odot}|} \tag{9}$$

where $K^* = (4.57 \times 10^{-6} N/m^2)\frac{A}{m}Q_{ab}$, being A and m the cross section area and the mass of the satellite and $Q_{ab} = 1$ is the absorption efficiency factor.

Figures 3 and 4 show the initial pair (ω,) and the maximum eccentricity reached in 250 years. The other initial elements are a = 26,559.74 km, e = 0.005, and I = 56.06°. We consider two values for the inclination of the Moon, I = 18.28° and 28.58°. We show that the initial value of the inclination is important, as shown in Figs. 3 and 4. The two straight lines represent the exact condition $2\omega + \Omega = 0$. Note that now we have added the Moon to our system, so that its effects can enhance the time variation of the eccentricity. The very smooth behavior (eccentricity-resonant angle) seen in Fig. 2 certainly will be lost as well as the position and the magnitude of the maximum and minimum values of the eccentricity. This is expected since now the satellite will be under the action of the disturbance of the Moon whose effect is about two times larger than the Sun. We also should point out that, in most of the cases shown in Figs. 3 and 4, the eccentricity does not reach high values in less than 200 years. Although this time is below 250 years, this is not acceptable in practical terms, because it increases the risk of collision between active and disposed satellites.

ISSN 2176-5480

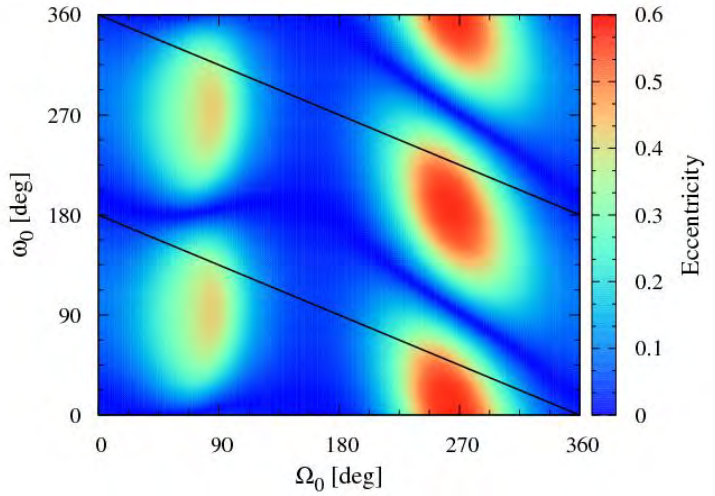

Figure 3. The color scale shows the maximum eccentricity reached in 250 year of evolution of the orbit of the satellite. Initial conditions: a = 26,559.74 km, e = 0.005, I = 56.06°. The straight line satisfies the relation $2\omega + \Omega = 0$. Initial inclination of the Moon is equal to 18.28°. The dynamics consider the exact system.

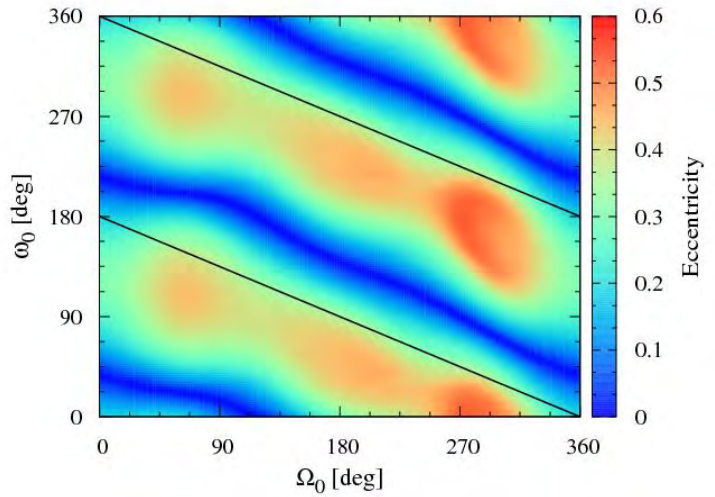

Figure 4. The same of the previous figure, but with I_L = 28.58°.

Figure 5 shows the results for a complete set of initial conditions of a GPS satellite (NORAD 22108) for the epoch April 4, 2012. The initial conditions of the Moon and the Sun are adjusted for the same epoch, because the initial conditions of the perigee of the Sun are significant. We note the growth of the regions with high eccentricities. However, again, in all cases the time for the eccentricity growth is very large (200 years). A more realistic condition requires not only the increase of the eccentricity, but the decay of the periapsis radius to values below than 6,978 km (periapsis altitude of 600 km). This value depends on the area to mass ratio of the satellite (Campbell et al., 2001). Therefore, in our simulations we are interested in obtaining sets of initial conditions that satisfy this precise concept, so that after some pre-fixed time, we can guarantee that the satellites really end up re-entering into the atmosphere of the Earth.

ISSN 2176-5480

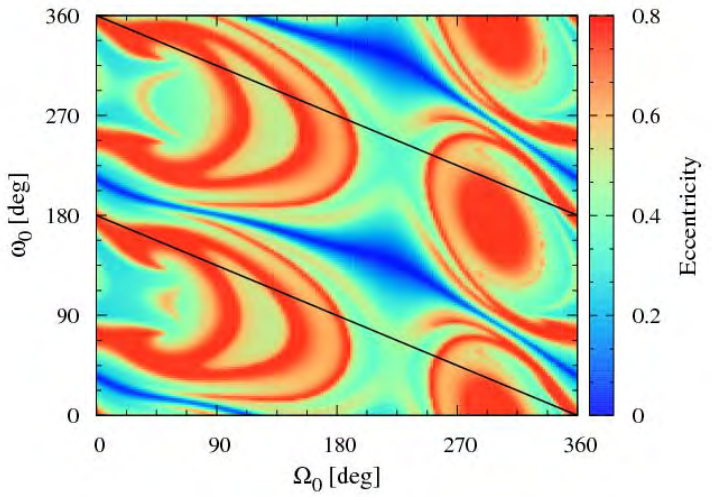

Figure 5. The same of Figs. 3 and 4. Initial conditions: a = 26,561.1206 km, e = 0.0220, I = 56.2641° (NORAD 22108). I_L = 21.78°, ω_{Sun} = 105.43° (Epoch 04/12/2012).

In an attempt to reduce the time that the eccentricity demands to reach high values, we decrease the initial value of the satellite apoapsis radius in 10,000 km with respect to its nominal value. The result is showed in Fig. 6. Opposite to what is desired, note that the region with high values of eccentricity almost vanished. This can be explained by our averaged model Eq. (5): the smaller is the semi-major axis (altitude), the weaker is the effect of the $2\dot{\omega} + \dot{\Omega} \approx 0$ resonance, that is, for satellites in lower orbits (small semi-major axis) the net effect of this resonance is negligible, in spite of its existence. Figure 6 clearly shows this fact. In this sense, we take an initial apoapsis radius 10,000 km above the nominal value. Figure 7 shows that the regions with high eccentricity are larger than in the previous figures, as expected.

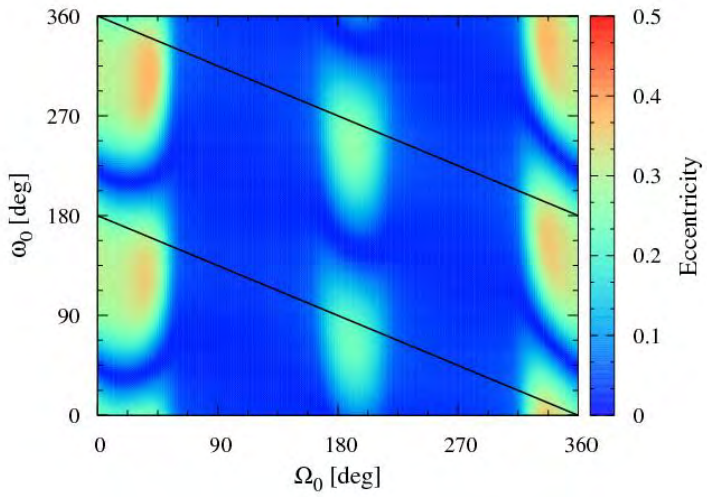

Figure 6. The same of Fig. 5, but with apoapsis radius 10,000 km below the nominal value.

ISSN 2176-5480

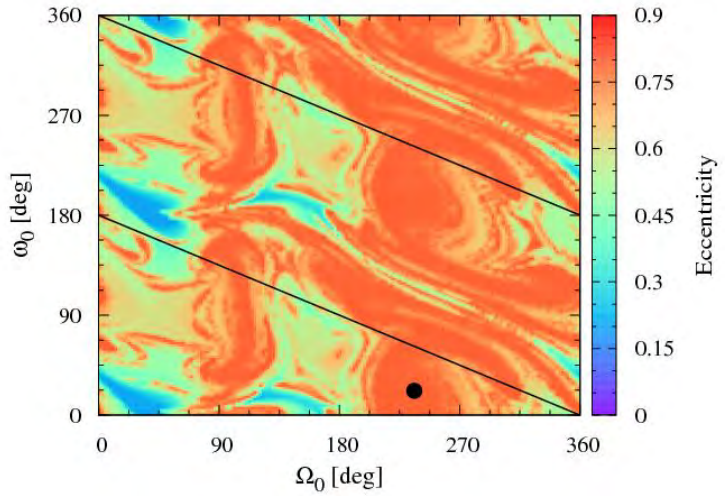

Figure 7. The same of Fig. 5, but with apoapsis radius 10,000 km above the nominal value.

As explained before, an analysis of which initial conditions in Fig. 7 drives the periapsis altitude to be below than 600 km is necessary. Figures 8 and 9 show the complementary information for that. Figure 8 shows the regions where the apoapsis altitude decreases to values less or equal than 600 km within 250 years. Comparing this figure with Fig. 7, we see that although the eccentricity can reach high values (0.8 for example), we see that this not enough to lower the periapsis altitude to penetrate into the atmosphere (in our case 600 km). Moreover, to decide the best initial pair (perigee and longitude of ascending node) to discard a satellite, we also need to consider the amount of time which will be spent by the satellite to reach 600 km of periapsis altitude. The search of these conditions is easily done directly from the simulations. In fact, fortunately, in the (ω, Ω) plane, the region covered by the conditions we are looking for is significant. In Fig. 9, in blue color, we have an interesting view of the main initial conditions. In Fig. 10, the time evolution of one specific orbit is given. Thus, increasing the semi-major axis of the satellite (via orbital transfer) so that the apoapsis radius raises, for example, 10,000 km above its nominal value, is a viable way to exploit the resonance to discard the GNSS satellites. In the next section we make a comparison of the cost (in terms of the increment of velocity) between the discard via resonance and the direct discard.

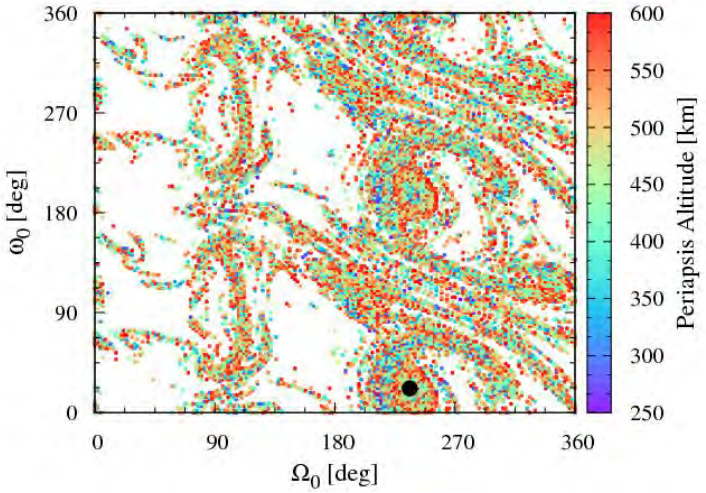

Figure 8. Initial conditions (ω, Ω) of Fig. 7 in which periapsis altitude has reached at least 600 km (or less). In the white regions the periapsis altitude does not reach 600 km in 250 years of integration.

ISSN 2176-5480

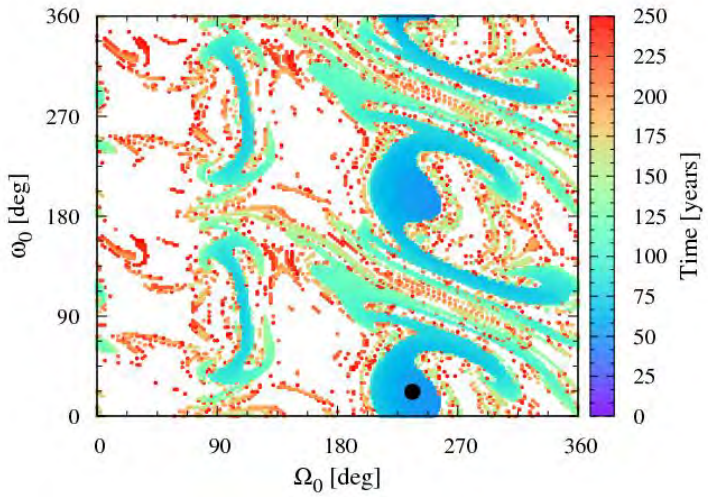

Figure 9. Time required for the periapsis altitude to reach 600 km in integrations of Fig. 7 as a function of the initial perigee and ascending node of the satellite. In the white regions the periapsis altitude does not reach 600 km during 250 years of integration.

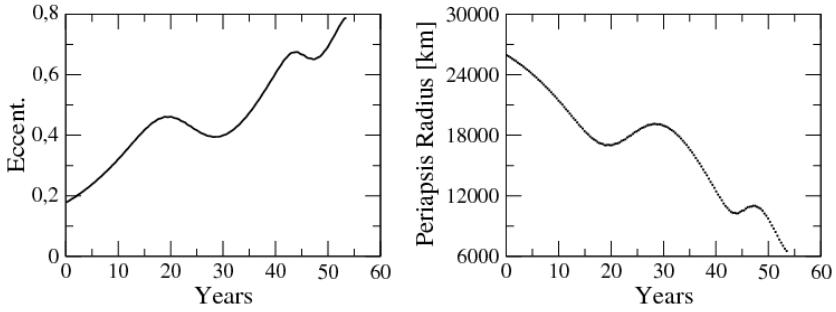

Figure 10. Temporal evolution of the eccentricity (left) and the periapsis radius (right) of a satellite with initial conditions: a = 31,557.9896 km, e = 0.17698, I = 56.2641, ω = 22°, and Ω = 236° (marked by a black circle in Figs. 7, 8, and 9). The periapsis altitude reaches 600 km after 50 years.

4. THE DIRECT DISCARD COMPARED WITH THE DISCARD VIA RESONANCE

The transfers chosen for the direct discard and for the increase of the semi-major axis in the technique of discarding via resonance are both of the Hohmann type (Vallado, 2007) because, in both cases, they are the simplest and fastest solution.

Classically, the Hohmann transfer is coplanar, and consists in the application of two increments of velocity Δv: the first one (Δv_a) at the periapsis of the initial orbit (point A, in Fig. 11) that puts the satellite in the transfer orbit (dashed), and the second one (Δv_b) applied at the apoapsis of the transfer orbit (point B) that puts the satellite in the final orbit, which have apoapsis coincident with the one of the transfer orbit.

Some differences appear between the original Hohmann transfer and the transfer that we use. Both orbits (initial and final) are elliptical in our transfer, including the one for the direct discard. The transfer occurs from point B to point A, and the second Δv does not exist, because we consider that the satellite has already entered in the atmosphere. Δv_b is in the direction opposite to the motion of the satellite. For the discard via resonance, the transfer occurs from the point A to point B, but Δv_b is not required, because this transfer is performed only to increase the apoapsis of the initial orbit.

ISSN 2176-5480

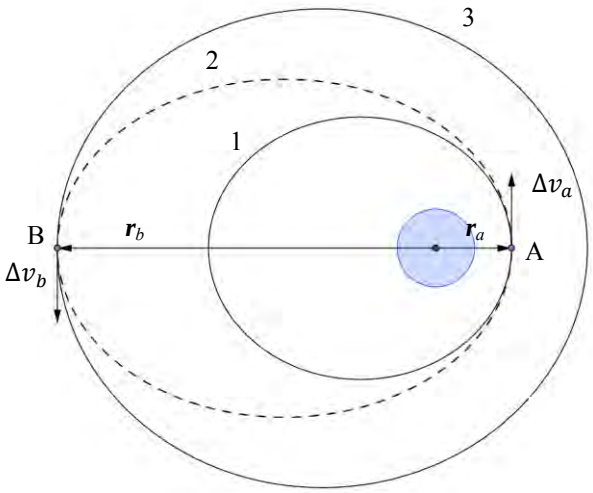

Figure 11. Geometry of the Hohmann type transfer.

For the direct discard, the apoapsis radius and the velocity at the point B of the orbit 3 are given by:

$$r_b = a_3(1 + e_3), \tag{10}$$

$$v_b = \sqrt{\frac{2\mu}{r_b} - \frac{\mu}{a_3}}, \tag{11}$$

where a_3 and e_3 are the semi-major axis and the eccentricity of the orbit 3 and μ is the gravitational parameter of the Earth.

The periapsis radius (r_a) is the equatorial radius of the Earth and the apoapsis radius coincides with the apoapsis of the orbit 3. Thus, we can calculate the eccentricity e_2, the angular momentum (H), and the velocity in the apoapsis (v_2) of the orbit 2 (Curtis, 2005):

$$e_2 = \frac{r_b - r_a}{r_b + r_a}, \tag{12}$$

$$H = \sqrt{r_a \mu (1 + e_2)}, \tag{13}$$

$$v_2 = \frac{H}{r_b}. \tag{14}$$

The increment of velocity in B (and consequently the increment to perform the direct discard), is:

$$\Delta v_b = v_b - v_2. \tag{15}$$

Table 1 shows the results of the direct discard transfers applied on some elements of the GNSS that have inclinations around 56° and that resides in MEO. The initial conditions was collected in the Celestrak Catalog (2012) and correspond to April 18, 2012 epoch. The initial conditions of the Sun and the Moon also correspond to the same epoch. The NORAD number is the satellite identification, a_0, I_0, e_0 are the semi-major axis, inclination and eccentricity of the initial orbit, Δv is the increment of velocity to execute the transfer, T is the period of transfer, and e the eccentricity of the final orbit. Figure 12 presents the tridimensional representation of the transfers for the satellites 20959 and 22014, where x, y and z are the components of the vector radius of these satellites, in km.

Table 1. Results for the direct discard transfers.

NORAD	a_0 [km]	I_0 [degree]	e_0	Δv [km/s]	T [h]	e
20959	26560.7664	54.5454	0.011944	1.44298304067	2.9633	0.6164
22014	26560.1638	56.3669	0.020705	1.42793604813	2.9944	0.6191
22108	26561.1206	56.2641	0.022017	1.42568876224	2.9993	0.6195
22700	26559.8276	56.4089	0.017141	1.43388624044	2.9818	0.6180

ISSN 2176-5480

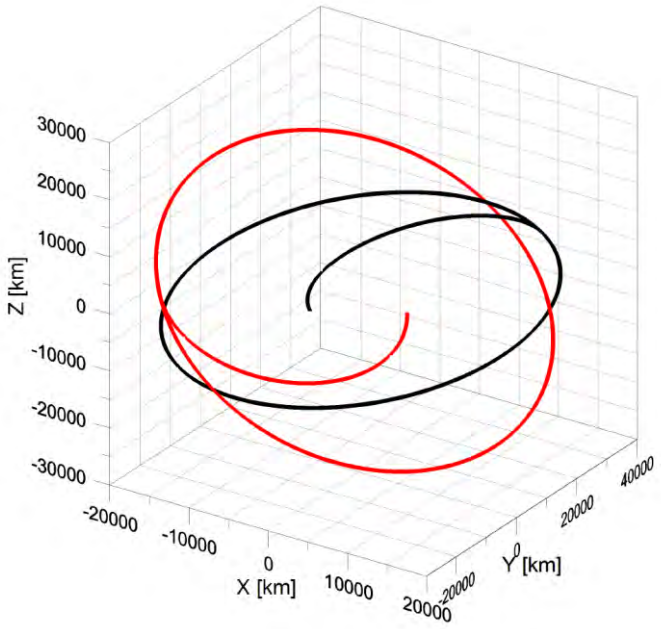

Figure 12. Tridimensional representation of the Hohmann type maneuver executed for the satellites 20959 (black) and 22014 (red).

The procedure to calculate the Δv to increase the apoapsis in the discard via resonance is quite similar to the previous calculation, and is omitted here. The final orbit in this case is the most eccentric orbit and this fact increases the solar perturbation. The limit to increase the apoapsis radius would be such that the correspondent Δv would be equal to the Δv spent in the direct discard and such that the final orbit does not cross the GEO. Table 2 shows some results of this transfer for the satellite NORAD number 22108, where Δr_{apo} is the increment in the apoapsis radius, a_f and e_f are the final semi-major axis and eccentricity, T is the transfer time, and Δv is the velocity increment that has to be applied to the satellite. The adjustment in the values of ω and Ω occur without any cost, because these angles have precession, and the discard could be planned when their values reach the desirable ones.

Table 2. Results of the discard via resonance transfer.

Δr_{apo} [km]	a_f [km]	e_f	T(h)	Δv [km/s]
10000	31557.98957	0.17699	7.7489	0.2896220183
15000	34057.98957	0.23740	8.6877	0.3973314563
20000	36557.98957	0.28955	9.6617	0.4882128746
25000	39057.98957	0.33503	10.6695	0.5659710974
30000	41557.98957	0.37503	11.7101	0.6332858627

Comparing the Δv required by the direct discard with the Δv required by the discard via resonance, we can note that the most economical strategy is the discard via resonance, even for high values of Δr_{apo}.

To show the entire process of the discard via resonance, we take, as an example the case with 10,000 km of Δr_{apo}. From Figs. 8 and 9 we can choose the initial pair (ω,Ω) that makes the satellite to reach 600 km of periapsis altitude in the shortest time. This pair must be chosen as close to the current pair of the satellite as possible, because in this way, we have to wait less time for the satellite to reach the desirable value of (ω,Ω) due to the natural precession of ω and Ω. When these values are reached, the maneuver to increase the apoapsis radius is performed, raising the apoapsis radius by 10,000 km. The consequence of this process is to place a satellite in a more eccentric orbit (natural consequence of the maneuver), which reaches 600 km of periapsis altitude in 50 years. This time is comparable with the time that the upper stages of the rockets that send the satellites Beidou and Galileo into orbit takes to reenter in the atmosphere of the Earth (Anselmo and Pardini, 2011).

We can decrease the time of discard by taking other values of Δr_{apo} keeping the same values of ω and Ω from Fig. 9. Figure 13 shows the time in which the periapsis radius reaches the value of 600 km of altitude during the numerical integration for several values of Δr_{apo}. We can verify that, if we take a pair (ω,Ω) in the unstable region of Fig. 8 (and consequently Fig. 9) and increase the apoapsis radius, the time of discard is reduced. However, from Δr_{apo} equal to 18,000, the time has an erratic distribution, which leads to an optimum value of Δr_{apo} around 10,000 km.

ISSN 2176-5480

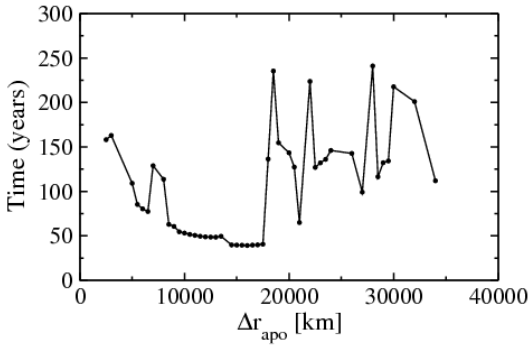

Figure 13. Time required for the periapsis radius to reach 600 km of altitude as a function of the Δr_{apo}.

5. CONCLUSIONS

We found an alternative method to discard the satellites of the GNSS which are in MEO and have inclinations around 56°, by using the resonance $2\dot{\omega} + \dot{\Omega} \approx 0$ and an orbital transfer to increase the apoapsis radius of the satellite to be disposable. We found sets of initial conditions such that the eccentricity of the satellite reaches high values, usually in less than 250 years. In comparison with the direct discard, the alternative method takes advantage, in terms of fuel expenditure. That is showed in terms of the increment of velocity that has to be applied to the satellite. The time required for the disposal is clearly shorter when compared to the time required to dispose the upper stages of rockets. Our technique provides the initial conditions which lead to high values for eccentricity of the orbit of the satellite much faster than those presented in previous work. The additional information of Figs. 8 and 9 guarantee the reentry in the atmosphere in the shortest possible time.

Although the focus of our work are the MEO satellites of the GNSS, and since the eccentricity grows faster when the satellite is closer to the Sun, we wonder on the long stability of the members of the Beidou constellation. Their inclinations are close to 56° and they are in the GEO region. The effects of the resonance $2\dot{\omega} + \dot{\Omega} \approx 0$ may be more intense for satellites in GEO, increasing possible risks of collisions.

6. ACKNOWLEDGEMENTS

The authors thank CAPES (Federal Agency for Post-Graduate Education - Brazil), CNPq (National Council for Scientific and Technological Development) and FAPESP (São Paulo Research Foundation). This research was supported by resources supplied by the Center for Scientific Computing (NCC/GridUNESP) of the São Paulo State University (UNESP).

7. REFERENCES

Allan, R. R., 1967. "Resonance Effects Due to the Longitude Dependence of the Gravitational Field of a Rotating Primary". *Planetary and Space Science* Vol. 15.

Anselmo, L. and Pardini, C., 2011. "Orbital Evolution of the Upper Stages Used for the New European and Chinese Navigation Satellite Systems". *Acta Astronautica* Vol. 68.

Beaugé, C. and Ferraz-Mello, S., 1994. "Capture in Exterior Mean-Motion Resonance Due to Poynting-Robertson Drag". *Icarus* 110.

Campbell, S., Chao, C. C., Gick, A. and Sorge, M., 2001. "Orbital Stability and Other Considerations for U. S. Government Guidelines on Post-mission Disposal of Space Structures". In *Proceedings of the Third European Conference on Space Debris*. Darmstadt, Germany. Ed.: Huguette Sawaya-Lacoste. ESA SP-473, Vol. 2, Noordwijk, Netherlands: ESA Publications Division.

CELESTRAK, On Line Satellite Catalog (SATCAT). CSSI, 2012. Available at <http://celestrak.com/>. Last access in April 18, 2012.

Chao, C. C., 2000. "MEO Disposal Orbit Stability and Direct Reentry Strategy". *Advances in Astronautical Sciences* Vol. 105.

Chao, C. C. and Gick, R. A., 2004. "Long-term Evolution of Navigation Satellite orbits: GPS/GLONASS/GALILEO". *Advances in Space Research* Vol. 34.

Curtis, H. D., 2005. *Orbital Mechanics for Engineering Students*, Elsevier Butterworth-Heinemann.

Everhart, E., 1985. "An Efficient Integrator that Uses Gauss-Radau Spacing". *Dynamics of Comets: Their Origin and Evolution*, 185.

ISSN 2176-5480

Ferreira, L. D. D. and Vilhena de Moraes, R., 2009. "GPS Satellites Orbits: Resonance". *Mathematical Problems in Engineering* Vol. 2009, Article ID 347835, doi:10.1155/2009/347835.

Gick, R. A. and Chao, C. C., 2001. "GPS Disposal Orbit Stability and Sensitivity Study". *Advances in Astronomical Sciences* Vol. 108.

Jenkin, A. B. and Gick, R. A., 2005. "Dilution of Disposal Orbit Collision for the Medium Earth Orbit Constellation". In *Proceedings of the 4th European Conference on Space Debris (ESA SP-587) – ESA/ESOC 2005*. Darmstadt, Germany.

Jenkin, A. B. and Gick, R. A., 2006. "Collision Risk Posed to the Global Positioning System by Disposed Upper Stages". *Journal of Spacecraft and Rockets* Vol. 43, No. 6.

Kuga, H. K., Medeiros, V. M. and Carrara, V., 1983. *Cálculo Recursivo da Aceleração do Geopotencial*, São José dos Campos, INPE (INPE-2735-RPE/433).

Lanczos, C., 1985. *The Variational Principles of Mechanics*. Univ. Toronto Press, 4th edition.

Mignard, F., 1991. "Effects of Radiation Forces on Dust Particles in Planetary Rings". *Phys. Dyn. Minor Bodies*.

NASA Safety Standard, 2005. *Guidelines and Assessment Procedures for Limiting Orbital Debris*, Washington, DC: Office of Safety and Mission Assurance (NSS 1740.14).

Pardini, C. and Anselmo, L., 2012 "Post-disposal Orbital Evolution of Satellites and Upper Stages Used by the GPS and GLONASS Navigation Constellations: the Long-term Impact on the Medium Earth Orbit Environment". *Acta Astronautica* Vol. 77.

Rossi, A., 2008. "Resonant Dynamics of Medium Earth Orbits: Space Debris Issues". *Celestial Mechanics and Dynamical Astronomy* Vol. 100.

Sanchez, D. M., Yokoyama, T., Brasil, P. I. O. and Cordeiro, R. R., 2009. "Some Initial Conditions for Disposed Satellites of the Systems GPS and Galileo Constellations", *Mathematical Problems in Engineering Volume 2009*, Article ID 510759.

Vallado, D. A., 2007. *Fundamentals of Astrodynamics and Applications*. Hawthorn: Space Technology Library.

Vilhena de Moraes, R., Fitzgibbon, K. T. and Konemba M., 1995. "Influence of the 2: 1 Resonance in the Orbits of GPS Satellites". *Advances in Space Research*, Vol. 16, Nº 12.

Yokoyama, T., 1999. "Dynamics of some fictitious satellite of Venus and Mars". *Planetary and Space Science* Vol. 47, Issue 1.

8. RESPONSIBILITY NOTICE

The authors are the only responsible for the printed material included in this paper.